RSC Advances

PAPER

View Article Online
View Journal | View Issue

Cite this: *RSC Adv.*, 2024, **14**, 25728

Fabrication and characterization of natural fiber reinforced cowpea resin-based green composites: an approach towards agro-waste valorization

Shruti S. Pattnaik,[a] Diptiranjan Behera,[a] Nigamananda Das,[a] Ashwini K. Dash[b] and Ajaya K. Behera *[a]

Received 14th May 2024
Accepted 2nd August 2024

DOI: 10.1039/d4ra03546a

rsc.li/rsc-advances

A paradigm shift towards using bio-resins or bio-derived resins among materials scientists has led to wide exploration of the sector. Polymers such as soy protein isolate, poly(hydroxy alkanoate), poly(lactic acid), and thermoplastic starch are all synthetically modified bio-based resins and are costly. The cowpea-derived resin with the least chemical modification was used in this study as a matrix for the formation of composites with natural fibers at a lesser cost. Fabrication of composites of vetiver and jute with varying weight percentages of fiber (50, 60, and 70%) in the innovative cowpea resin resulted in favorable mechanical properties and degradability. The tensile strength was the highest for the jute-cowpea composite (JCP2) at around 37.49 MPa, which also has a flexural strength of 40.3 MPa. Dynamic mechanical analysis of composites reflects the moderate storage moduli of 1802 MPa for JCP2 and 1351 MPa for vetiver-cowpea (VRCP2) composites. Impact strength studies and thermal stability also show optimistic results. The contact angle, water absorption behavior, and swelling in thickness show the moderate hydrophobicity of the composites. This is also a reason for the improved degradability of the composites in soil-burial and microbial environments. Characterizations such as FE-SEM and FTIR spectroscopy, conducted after the degradation of the samples, showcased the level of deterioration. All these results suggest using the innovative cowpea resin as a good alternative to various other synthetic thermoplastic resins used in the fiber reinforced composite manufacturing field.

1. Introduction

Plastic pollution is a menace as the accumulation of plastic materials in the environment, particularly in water bodies and soil, occurs for a very long time because of their high stability under thermal, physical, and chemical stress conditions. Even if the larger plastic particle breaks down, it produces microplastics, which are very tiny plastic particles that remain persistent in our surroundings, leading to health hazards. To mitigate these risks, a paradigm shift towards bioplastics has occurred among materials scientists. Bioplastics are either sourced from nature, hence reducing the load on fossil fuels, or break down into eco-friendly sub-particles/molecules that add value to the soil.[1–3]

Recently there has been a growing interest in the valorization of agro-waste and agro-derived chemicals into useful bioplastics, which are non-toxic, cheap, and reduce the burden on solid waste management.[2,4] Biomolecule polymers such as starch, proteins, and oils have been extensively explored for such advancements.[5] For example, processing of corn-kernel derived zein protein with glycerol and glutaraldehyde was reported to develop packaging materials with good barrier, mechanical, and thermal properties. The optimum properties were obtained for 25 wt% of glycerol and 1 wt% of glutaraldehyde.[6] Similarly, moist food packaging materials were developed using gelatin and zein composites with glycerol. The comparatively hydrophobic nature of zein endows the composite with lesser water solubility and improved crystallinity, hence suggesting a possible alternative to classical polyethylene.[7] Various research studies on bioproducts made by thermoplastic processing of gluten derived from wheat have also been reviewed.[8] As raw proteins do not possess the characteristics of plasticization by thermal processing, the need for plasticizers and compatibilizers is inevitable here. The use of soy-protein isolates (SPIs) to modify urea-formaldehyde resin adhesives in fiber-board panels is reported, as it reduces the emission of free formaldehyde pollutants to the environment.[9]

Another legume seed that is widely popular in tropical and subtropical regions is cowpea (*Vigna unguiculata*). The world produces around 8.9 million metric tons of cowpeas, by 2019, as per the reports, which are a good source of protein and essential amino acids, with less contribution of lipids.[10] They have a wide range of varieties like black, red, cream, brown-eyed, black-eyed,

[a]*Department of Chemistry, Utkal University, Bhubaneswar, Odisha 751004, India. E-mail: ajayabehera@utkaluniversity.ac.in; Fax: +9106742581850; Tel: +918280098214*

[b]*Department of Fashion Technology, OUTR, Bhubaneswar, Odisha 751029, India*

etc., which differ slightly in their nutritional values as well. The black-eyed cowpea seeds contain a proximate protein composition of 23.52 g and around 60 g of carbohydrates, in 100 g of seeds.[11] Essential amino acids like phenylalanine, leucine, lysine, valine, *etc.* are present in these seeds, except the sulphur-containing ones-methionine and cysteine.[11,12] However, the quantities of these nutrients fall below the nutritional standards prescribed by the WHO for infants and children.[13] So, isolates of these proteins and starches are of more use. Methods like ultrasound and hydrothermal treatment are used to improve the starch's physico-chemical properties, by decreasing the branching of amylopectin. This helped in the better digestibility of the starches when used in the processing of food products.[14] Protein isolates from dehulled, defatted cowpea flour were extracted by forming a suspension and centrifugation, which could be further used in the food industry.[15]

However, marked down, infected cowpea seeds become unfit for human consumption and add up to the waste. So, alternative bioproducts like biofilms and composites made out of this agro-waste could work wonders. Hewage *et al.* formulated cowpea protein isolate biofilms using polyethylene glycol and glycerol in different w/v%, at different pH, which had good resistance to permeability and decent mechanical strength.[16] A report on the use of cowpea husk in addition to clay for fabrication with unsaturated polyester is also presented.[17] The reinforcement improved the hardness and damping properties but reduced the tensile and flexural strength. Further addition of lignocellulosic wastes or other bio-compatible fibers as a reinforcement to biopolymers like PLA, SPI, TPS, *etc.* suggests further scope for biomass valorization.[18–21] These are non-persistent in the ecological system after degradation, along with providing alternatives to conventional fossil-sourced chemicals. However, the cost-efficiency decreases due to manifold chemical modifications.

In our studies here, we have tried to substantiate the use of bioresin made out of black-eyed cowpea milk, with lignocellulosic fiber reinforcements to improve the mechanical attributes. Two such fibers of interest are jute (*Corchorus capsularis*) and vetiver (*Chrysopogon zizanioides*), which are widely found in the South-Asian subcontinent. They have been fabricated into various composites with thermoplastic and thermoset resins like epoxy, polypropylene, polystyrene, polyester, *etc.*, where the matrix material is rarely degraded.[22,23] But their use with cowpea milk-based resin, which is completely degradable, hasn't been reported, to our knowledge. So, we have conducted various tests and experiments to investigate the use of these biocomposites and hence determine their future scope.

2. Materials, processing and characterization

2.1. Materials

Old nonwoven jute felts and vetiver fiber mats, which are used as summer screens in houses, were sourced locally from Bhubaneswar (Odisha, India) markets. Marked-down black-eyed cowpea seeds, without the bean pod, were bought from a local grocery mart in Bhubaneswar. Polyethylene glycol (PEG-400) and glutaraldehyde, which were utilized as plasticizing agents and crosslinkers in resin curing, respectively, were resourced from SRL, India. Other minor-use chemicals like NaOH, KBr, and CH_3CH_2OH too were procured from SRL, India.

2.2. Processing

2.2.1. Surface improvement of jute and vetiver fiber-mat. Nonwoven jute felts and vetiver root fiber mats were thoroughly scrubbed under running tap water to scour off the dirt and unwanted particles. They were again cleaned with de-ionized water to remove tap-water impurities that may be present, followed by drying under a hot-air oven at a temperature of 55–60 °C to achieve a constant weight. The fibers were submerged in sodium hydroxide solution made of 2% by weight, for 2 hours at room temperature (30 ± 2 °C) to remove the pectin and wax present on the surface.

2.2.2. Synthesis of cowpea resin. Black-eyed cowpea seeds were soaked in distilled water in a ratio of 1 : 4, overnight (around 6 hours) at room temperature. The hulls were then separated with gentle pressing and ground in a household grinder to make a flowy paste-like consistency, without adding extra water. This paste was then squeezed using a muslin cloth to extract out the milk.[23] The solid content of the milk was calculated and found to be roughly around 20% at a pH of 7.2.[3,23]

To increase the plasticity of the cowpea resin (CPR), 10 wt% (optimized w.r.t to the solid content of milk) of polyethylene glycol (PEG-400) was stirred at 500 rpm with the extracted cowpea milk for 1 hour.[22] To this 10 wt% of glutaraldehyde as a cross-linking agent was added and stirred for 5 more minutes.[22] The cured resin was then directly used to fabricate the composites.

2.2.3. Fabrication of jute-cowpea and vetiver-cowpea composites. For the preparation of the jute-cowpea (JCP) composite, nonwoven jute felts (400 gsm) (15 cm × 15 cm) were employed as the reinforcement material. Different composites were created and labeled as JCP1, JCP2, and JCP3 by varying the weight percentage (50, 60, and 70%) of jute fabrics, respectively. The cured cowpea resin (with glutaraldehyde and PEG-400) was poured on fibers for fabrication in 50, 40, and 30 wt%, accordingly. The cowpea resin-dipped jute fibers were then 70–80% air-dried in a hot air oven at around 55 °C for 60 minutes (or can also be left for normal air-drying at room temperature for 5–6 hours, until the resin stops excessive dripping).[23] These fibers now have around 30% moisture left. To manufacture the composites, the coated fabrics were pressed together at a temperature of 130 °C for 15 minutes at an optimized pressure of 25 kg cm^{-2} in a hydraulic press.[23] Similarly, to make vetiver reinforced cowpea (VRCP) (VRCP1-VRCP3) composites, different weight percentages (50, 60, and 70) of vetiver root fibers were used as the reinforcing material with the cowpea resin. Fig. 1 displays the diagrammatic representation of the scheme for the synthesis of cowpea resin film, and the digital images of fabricated VRCP and JCP composites.

2.3. Characterization

2.3.1. Carbohydrate and protein content evaluation for the extracted cowpea milk. The anthrone-sulphuric acid technique

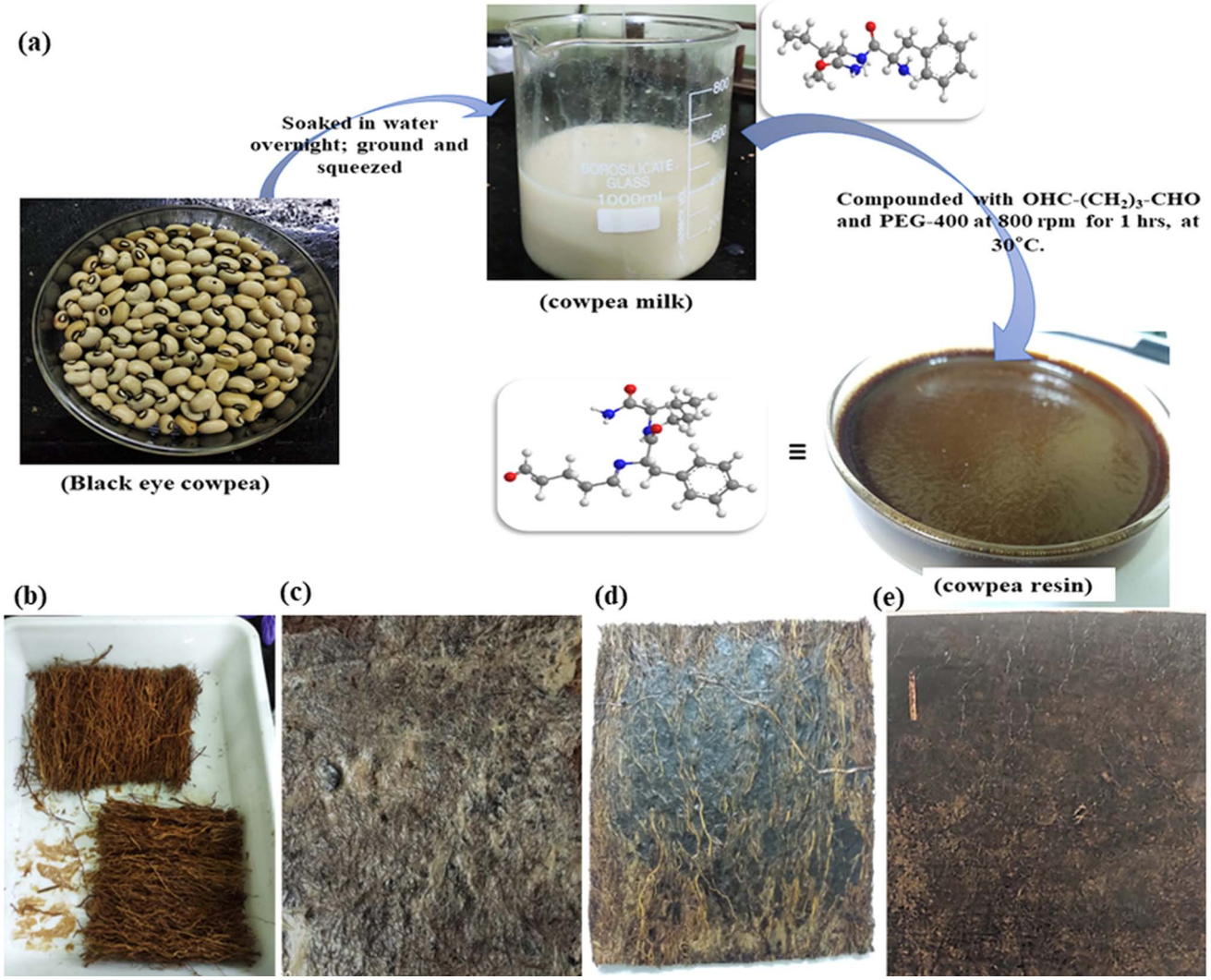

Fig. 1 (a) Diagrammatic representation of the scheme for the synthesis of cowpea resin film and digital photographs of (b) alkali-treated vetiver root fiber, (c) alkali treated jute felt, (d) VRCP composite, and (e) JCP composite.

quantified the overall carbohydrate content in the milk sample. Different concentrations of cowpea milk samples were combined with sulfuric acid and anthrone reagent, followed by boiling until the reaction completed. After cooling, the solution's absorbance was assessed at 620 nm through a UV-vis spectrophotometer (Agilent Cary 100, USA). About 5 different concentrations were prepared to run the experiment.

Bradford assay was utilized for the quantification of protein in the extracted milk. 5 known concentrations of the milk samples were prepared with the bovine serum albumin standard in phosphate buffer. The samples were then vortexed with Bradford assay containing Coomassie Brilliant Blue G-250 dye, allowing the dye to bind. The absorbance of the prepared samples and the standard was observed at 595 nm in the same UV-vis spectrophotometer and the acquired data were plotted to determine the unknown protein concentration by interpolation.

2.3.2. Density and void fraction of composites. The fabricated composites' void fraction was measured following ASTM D2734-91. The matrix and fiber are the two fundamental components of the composites under examination. The following equation (eqn (1)) is used to determine the theoretical density (ρ_t) of composites in proportion to the weight ratio.[24]

$$\text{Theoritical density } (\rho_t) = 100 \Big/ \left[\frac{r}{d_r} + \frac{f}{d_f}\right] \quad (1)$$

where r = resin content (wt%), d_r = resin density (g cm^{-3}), f = fiber content (wt%), and d_f = fiber density (g cm^{-3}). By merely computing the volume and the dimension ratio, the composite's accurate density (ρ_e) was established.[24] For various composites, the volume fraction of voids ($\varnothing_v$) was estimated using eqn (2).

$$\text{Volume fraction } (\varphi_v) = \frac{\rho_t - \rho_e}{\rho_t} \quad (2)$$

2.3.3. Tensile and flexural property measurement. ASTM D638-03 [ASTM (2003)] and ASTM D790-03 standards were complied with, for the testing of tensile and flexural properties

of the fabricated composites using the universal testing machine (INSTRON 68FM-300 UTM, USA). The test sample size was kept at 64 × 12.7 × 3.2 mm^3 and the cross-head parameter was set at 5 mm min^{-1}.[23] An average of 8 similar specimen observation results was considered for the properties. In the case of flexural properties, the speed parameter for the cross-head was kept at 2 mm min^{-1}, and similar data accumulation was carried out.[23]

2.3.4. Dynamic mechanical analysis. Mechanical performances of the JCP2, VRCP2, and CPR blends in a dynamic temperature setting were noted through an analyzer instrument (NETZSCH DMA 242, Germany). A fixed frequency of 1 Hz and a heat transmission rate of 10°C min^{-1} were adopted in the solitary cantilever function during the investigations. A temperature array (35 to 200 °C) was maintained for the test specimens of sizes 40 mm × 10 mm × 3 mm.

2.3.5. Impact strength analysis. An Izod impact instrument (S. C. Dey & Co., India) was deployed to test the impact durability of jute-cowpea and vetiver-cowpea composites. The temperature parameters were kept at 30 ± 2 °C, by following the standards mentioned in ASTM D256-97 [ASTM, (1997)]. The average impact value was assigned based on testing five samples associated with all the composite formulations.

2.3.6. Contact angle measurement. An SEO contact angle meter (SEO K100, Germany) was utilized for determining contact angle as a means to investigate the hydrophilic characteristics of composites.[22] Using a micro-syringe, a droplet of water (1–2 μL) was applied to the material's surface, and a CCD camera connected to the device captured pictures for each measurement. The overall contact angle reading is provided after at least six measurements, for each sample, which were made on its surface at various locations.

2.3.7. Water absorption analysis. Jute and vetiver composites were evaluated by water sorption and thickness swelling tests to analyze their dimensional stability in complete water submergence conditions. As per the standards mentioned in ASTM D570-05, deionized water was used at room temperature (30 ± 1 °C), and the dimension parameters were kept at 60 × 50 × 5 mm^3. 5 repeat units were taken to report the data, for each formulation. Excess dripping water present on the surface was carefully wiped away by soft dabbing with tissue paper. Eqn (3) was employed for the calculation of the amount (%) of water absorption:[23]

$$\text{Water absorption}(\%) = 100 \times \frac{W_f - W_i}{W_i} \quad (3)$$

where W_i and W_f are the weights of the test sample before and after observation. Similarly, eqn (4) was employed to check the increment in thickness post the experiment.[23]

$$\text{Thickness swelling}(\%) = 100 \times \frac{T_f - T_i}{T_i} \quad (4)$$

where T_i and T_f are the measures of the width of the test specimen before and after the experiment.

2.3.8. Thermal analysis. The thermal endurance (onset degradation temperature) of the resin CPR, and the composites, JCP2 and VRCP2, was investigated using TG/DTG analysis (TGA-209F; Netzsch, Germany). Before testing, the samples were dried overnight at around 90–100 °C. Temperature parameters were set with the starting temperature at 35 °C and ending at 500 °C. The heating rate was kept at 10°C min^{-1} and the test was carried out in a nitrogen gas environment.

2.3.9. Biodegradation investigation

2.3.9.1 Degradation under composting conditions. The BIS1623-92 standard was complied with while carrying out soil burial tests for the decomposition of several composite formulations. The composting conditions were specifically formulated in a ratio of 1 : 1 : 2 for manure, sand, and humus-rich soil, respectively. The relative humidity of the composting condition at 30% and an ambient temperature of 30 ±1 °C were sustained throughout the experiment. The weight of the test samples was recorded before burial (W_0) and then they were laid deep into the compost bed and covered. The weight after regular intervals of time (7, 15, 30, 45, and 60 days) was noted post cleaning with water and desiccating them in a hot-air oven for about 5–6 hours. Eqn (5) was utilized to evaluate the loss percentage in terms of weight and triplicates of each formulation were averaged.[20]

$$\text{Weight loss}(\%) = 100 \times \frac{W_0 - W_1}{W_0} \quad (5)$$

2.3.9.2 Degradation under direct microbial conditions. In a BOD incubator, 20 μL of pre-cultured *Aspergillus niger* strain was added to sterilized potato dextrose broth and kept at 28 °C. After 72 hours of incubation, the desiccated and weighed specimens were placed into a glass conical flask containing the fungal strain. The samples were collected at regular intervals of 7, 15, 30, and 60 days, washed with ethanol to remove live masses, and then dried in an oven for approximately 6 hours. The composites' percentage weight loss was calculated using eqn (5), post deterioration.[20] Each sample was evaluated in triplicate, and an average weight decrease was considered for assessment.

2.3.10. Field emission scanning electron microscopic analysis. The microstructures of CPR, JCP, and VRCP composites were examined before and after different biodegradation using a FESEM (ZEISS, SUPRA-55, Germany) apparatus to understand the nature of the attack. The process parameters like an accelerating voltage of 5 kV, magnification of around 1.5–2k×, and coating of the sample with a thin layer of gold (to mitigate electrical charging and increase the resolution of imaging) were maintained for all specimens.

2.3.11. Fourier transform infrared (FTIR) spectroscopic analysis. The degree of deterioration in terms of loss/decreased intensities of essential functional groups in CPR, JCP, and VRCP composites was determined by FTIR analysis of their powdered samples, before and after their degradation, using an IR spectrometer (SHIMADZU IRAffinity-1S, Japan). The range of the spectra that were recorded was 400–4000 cm^{-1}. Before KBr pellets were made, the powder sample was vacuum dried for an hour at 90 ± 2 °C.

2.3.12. Statistical analysis. Statistical and variant analyses were performed using SPSS software (v19, IBM). To assess the significance of differences between the obtained results, one-way

ANOVA was conducted, followed by the Tukey HSD post-hoc test. A confidence level of 95% ($p < 0.05$) was applied in these analyses to determine statistical significance. The level of significance was tested for mechanical properties-tensile and flexural strength and moduli, along with the impact strength test.

3. Results and discussion

3.1. Carbohydrate and protein content evaluation for the extracted cowpea milk

In the case of the anthrone-sulphuric acid test for carbohydrate quantification, the amount of carbohydrates depends on the extent of colour shown by the samples upon complexation. The blueish-green colour obtained had a linear relationship with the amount of carbohydrates present in the milk sample. This test measures both reducing and non-reducing carbohydrates.

In the Bradford assay, the quantity of protein is dependent on the intensity of blue colour obtained, upon binding of the dye and proteins in the samples. The data in the case of both dehulled cowpea seed extracted milk and the ones with the hulls intact are presented in Table 1. The values adhere to different literature as well.[11]

3.2. Density and void-fraction of jute and vetiver cowpea composites

In JCP and VRCP composites, the volume proportion of voids is presented in Table 2, together with the calculated and observed densities. The void content of composite materials is the major variable that distinguishes the actual density values from theoretical ones. The mechanical properties of composite materials are strongly impacted by the existence of voids. Higher void contents reduce fatigue resistance and increase susceptibility to water infiltration.[24] Therefore, including the void content while evaluating the composites' quality is advantageous. The improved and adequate resin coating on the jute surface may have contributed to JCP2's reduced void content of 10.65% as compared to the other JCP composites. With an increase in jute content, the void content of the jute–cowpea (JCP3) composite slightly rose to 10.76%. This might be a result of the jute surface's insufficient coating by cowpea resin in JCP3. VRCP composites had higher void contents as compared to JCP composites, which may be the result of insufficient bonding between the fibers of vetiver root and cowpea resin, along with the thicker fibers of vetiver.[25]

Table 1 Carbohydrate and protein content in black-eyed cowpea milk

Sample	Carbohydrates (mg g^{-1})	Protein (mg g^{-1})
Cowpea milk without hull	570–595	203–220
Cowpea milk with hull	590–620	215–245

3.3. Mechanical property analysis

Fig. 2 sums up the mechanical characteristic analyses of all the formulations of JCP and VRCP. The tensile strength of JCP rose from 33.2 MPa to 37.49 MPa upon increasing the jute loading (from JCP1 to JCP2) along with an improvement of 20.56% in the tensile moduli for the same. The observed 19.9% increment in the flexural strength and nearly 6% increment in the bending moduli support 60 wt% jute fiber loading to be an optimum loading in the CPR matrix, hence suggesting better adhesive interactions between the jute fiber and cured CPR.[26]

Cellulosic hydroxyls from the fibers and proteinaceous amino and carboxylic acid groups of the resin can show a strong dipole–dipole/hydrogen bonding interface, leading to improved functionality mechanically (Fig. 3).[23] However, moving towards higher loading of fiber (for JCP3), the mechanical properties deteriorated probably due to insufficient wetting of the fiber with the CPR and hence weakening of the fabricated composite through vulnerable initiation and propagation of cracks.[26] The same applies to the vetiver-based composites too. The highest tensile strength for VRCP2 was about 36.2 MPa, with a modulus of 953 MPa. As evident from the data, the mechanical properties of jute composites in the CPR matrix were on a higher end in comparison to vetiver, with nearly a 5–10% improvement in all the attributes mentioned above. This superiority may be ascribed to various factors like fiber surface adhesiveness, high aspect ratio, and better alignment of the jute felt.[27] All the individual fiber loading (for one particular fiber type) was treated as an individual treatment, with the calculated p-value below 0.05, thus encouraging a substantial effect of 50, 60, and 70 wt% of fiber loading on the mechanical properties of the composite. Further results from the Tukey HSD post-hoc test suggest a significant gap for JCP2 and VRCP2 (both 60 wt%) in comparison to the other two fiber loadings, hence enhancing their properties.

3.4. Dynamic mechanical analysis of the fabricated composites

Dynamic mechanical analysis (DMA) is a technique used to measure the mechanical properties of materials as a function of

Table 2 Density and void fraction of JCP and VRCP composites

Composites	Fiber (wt%)	Measured density (g cc^{-1})	Theoretical density (g cc^{-1})	Volume fraction of voids (%)
JCP1	50	1.120	1.225	10.74
JCP2	60	1.159	1.298	10.65
JCP3	70	1.198	1.343	10.76
VRCP1	50	1.078	1.219	11.54
VRCP2	60	1.108	1.251	11.45
VRCP3	70	1.132	1.285	11.91

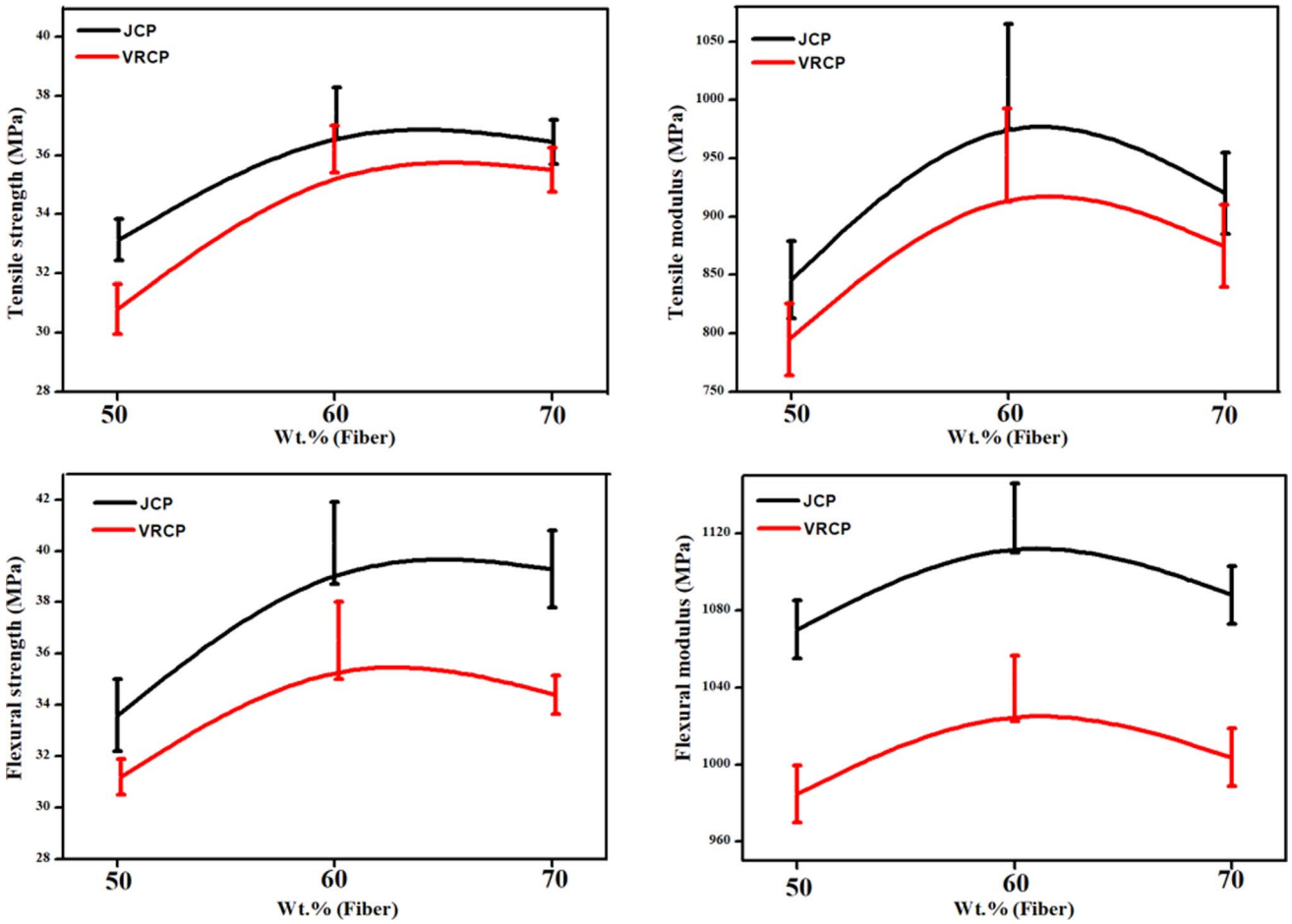

Fig. 2 Mechanical properties of fabricated JCP and VRCP composites: (a) tensile strength, (b) tensile modulus, (c) flexural strength, and (d) flexural modulus.

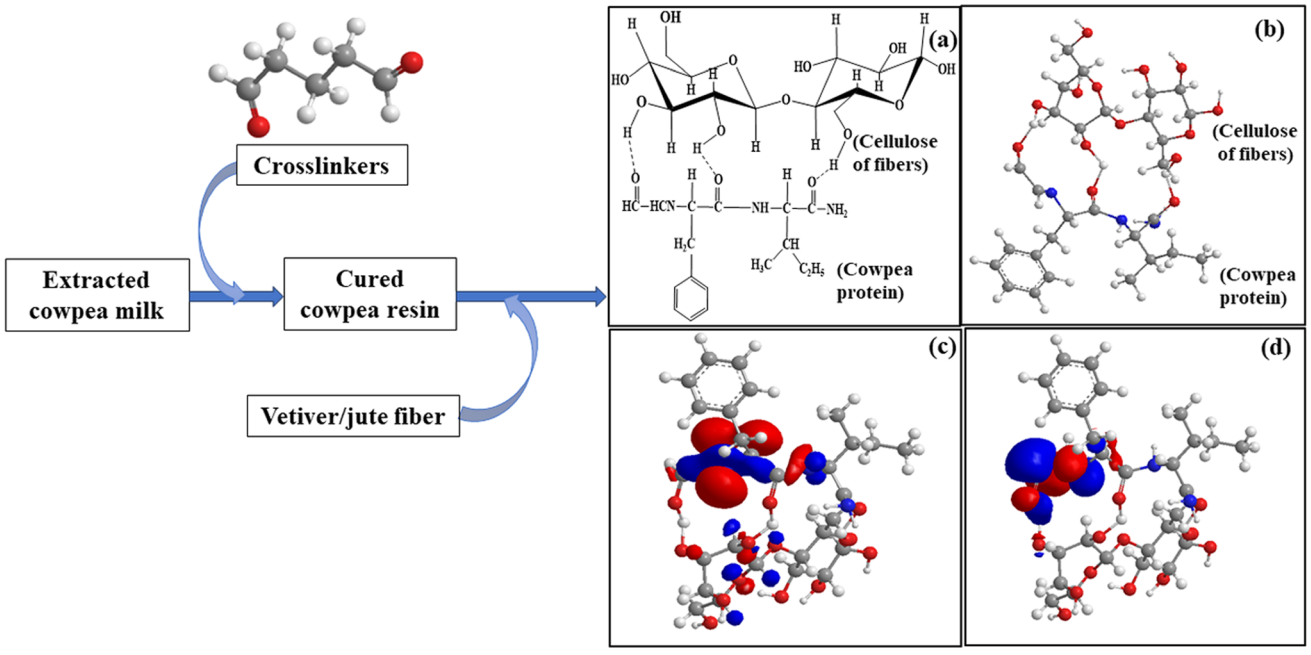

Fig. 3 A plausible representation of (a) the crosslinking of a short chain of amino acids from the cowpea matrix and natural fibers upon fabrication of the JCP and VRCP composites. (b) 2-D and 3-D representations of fiber's cellulose and resin's amino acid interaction, respectively. (c) and (d) demonstrates the HOMO and LUMO of the interacting sites, respectively.

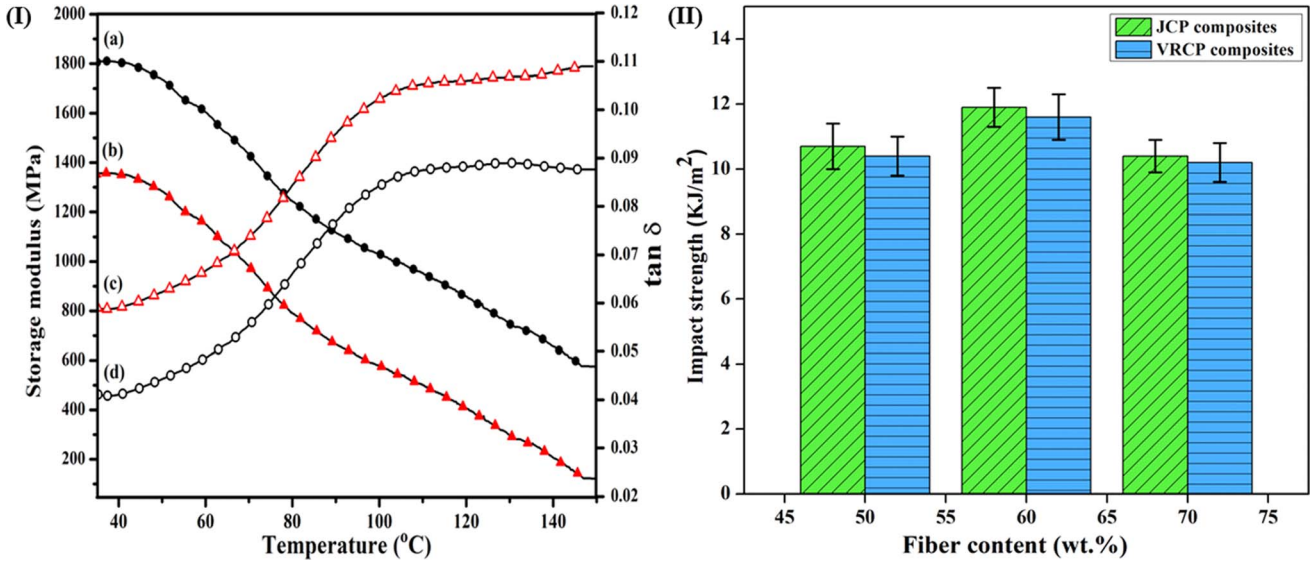

Fig. 4 (I) Storage modulus of (a) JCP2 and (b) VRCP2, tan δ of (c) VRCP2 and (d) JCP2, and (II) impact strength graph of JCP and VRCP composites.

temperature, frequency, or time under an oscillating load, as presented in Fig. 4(I). The storage modulus and the tan δ (damping factor) values were obtained to study the composite's stiffness and viscoelastic behavior, respectively.[26] The JCP2 composite shows a storage modulus value of 1802 MPa at 35 °C, whereas the VRCP2 has a value of 1351 MPa at the same temperature. This gives us an insight that the JCP2 is a stiffer composite and can store more amount of elastic energy. While considering the tan δ, the VRCP2 has a higher value (0.059) in comparison to JCP2 (at 0.041), which indicates that the molecular motion between the CPR resin and the vetiver fiber is more, leading to a loosened packing in VRCP2. Hence, we can conclude that the JCP2 formulation shows better performance than VRCP2 under oscillating load at varying temperatures.

3.5. Impact strength analysis

Fig. 4(II) illustrates the impact strengths of JCP and VRCP composites resulting from energy absorption during impact or shock loading. As the fiber content in the composites increases, a rise in impact strength occurs.[28] A higher force is needed to defibrillate the fibers and cause composite breakage with a definite increase in fiber loading. Among all JCP and VRCP composites, JCP2 displayed the highest impact strength at 11.9 kJ m^{-2}. Similarly, VRCP2 exhibited a fair performance at 11.6 kJ m^{-2}. This superiority is likely attributed to the superior adhesion between the finer thread-like jute fibers and matrix, enhancing energy absorption capacity in JCP2, as is evident from the significant p-value < 0.05 and followed by a Tukey HSD test.[29] However, the impact strength declined as the fiber content increased from 60 to 70 wt%. This decrease may be attributed to the lower amount of cowpea resin present, which fails to bind fibers effectively, leading to regions of stress concentration that require less energy to initiate cracking.[30] Consequently, JCP3 and VRCP3 demonstrated a decrease of 14.4% and 13.7% in impact values, respectively. JCP2 is acknowledged as the prime composite.

3.6. Extent of hydrophilicity and effect of water on the dimensional stability

The hydrophilicity of JCP and VRCP composites was studied by the angle of contact and the stability of dimensions of the formulated composites was studied through water absorption and swelling in thickness tests, as represented in Fig. 5(I and II). A higher contact angle signifies greater hydrophobicity in a composite, as substantiated by JCP2, with a contact angle of 67.5° compared to VRCP2's 65.2°, between the composite surface and the water droplet. This variance may stem from the enhanced number of linkages of cowpea resin to the rough surface of jute fibers, hence preventing easy water permeation.[22] The angle of contact for CPR is about 40.2°. Following water absorption, resin film thickness swelling is higher than in both sets of composites. After 24 hours, JCP2 and VRCP2 composites exhibit water absorptions of 55.1% and 57.08%, and thickness swelling values of 48.2% and 50.4%, respectively. Despite the inherent hydrophilicity of jute fibers, vetiver fibers, and CPR resin, there is a drop in water affinity for the cured composites because of the tight packing, hence reducing the contact surface.[23] Contact angle, water absorption, and thickness swelling measurements after a day's submersion reveal that JCP composites are more hydrophobic and stable in water as compared to their VRCP counterparts.

3.7. Thermal stability analysis

Fig. 5(III) presents the result of the thermogravimetric study of CPR, VRCP2, and JCP2 composites. An initial degradation of less than 10% is seen in all the samples below 100 °C, upon the loss of moisture. Inflection in dTG for CPR is obtained at 256.0–286.85 °C, with a broad peak suggesting the stability of the protein and starch until this stage of temperature. In the case of

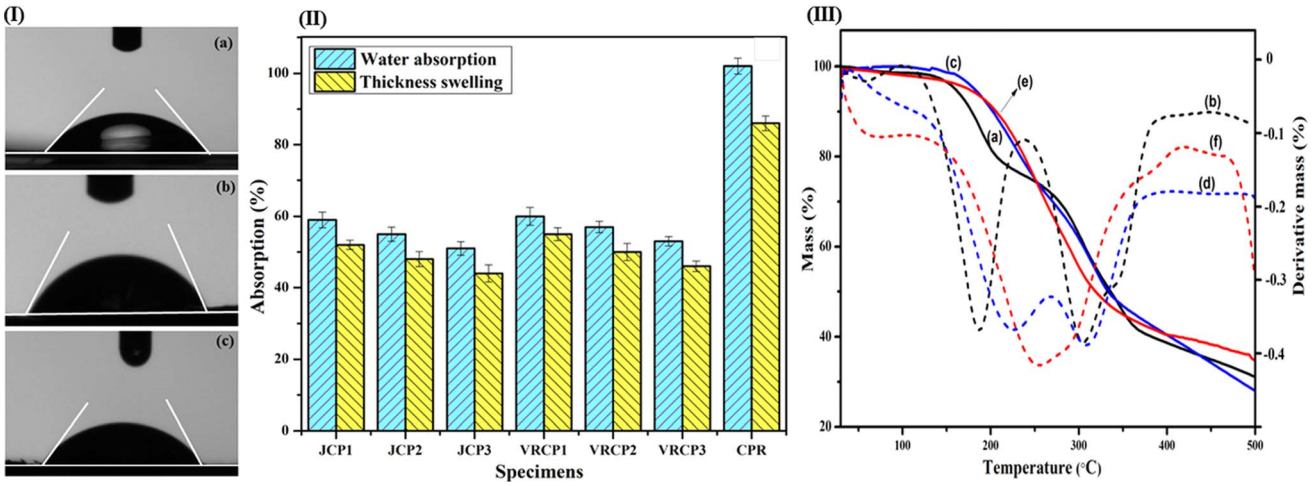

Fig. 5 (I) Contact angle measurement of (a) CPR, (b) JCP2, and (c) VRCP2; the effect of water on the stability of dimensions of the composites and resin through (II) water absorption and swelling in thickness for CPR, JCP (1–3), and VRCP (1–3), and (III) TG curves of (a) VRCP2, (c) JCP2, and (e) CPR, and dTG graphs of (b) VRCP2, (d) JCP2, (f) CPR.

the composites, the next inflection point (post-water loss) was observed at 187.40 °C (for VRCP2) and 223.69 °C (for JCP2), which is lower than that for resin.[31] This is due to the presence of hemicellulose, which lowers the thermal stability of the composite structure and degrades at this stage.[23] Post these, the third point of inflection is seen at 304.60 °C and 310.5 °C for VRCP2 and JCP2, respectively, and is positioned for the cellulosic part of the natural fibers. This last observation suggests the greater thermal stability of the JCP2 composite. A residual mass of about 28–31% is obtained for all the samples.

3.8. Degradation analysis of composites

3.8.1. Weight loss of composites in soil-burial and microbial environments. Fig. 6(a) and (b) represent the degradation in weight for the CPR film in comparison with all the JCP and VRCP composites in composting and microbial conditions, respectively. There is a significant loss of mass within 7 days of the experiment, in the compost bed. The soil microbes opt for cowpea's proteinaceous and starchy make-up, over cellulose and hemicellulose found in vetiver and jute, which results in massive degradation of the CPR film compared to the 2 sets of the composites.[26] Post 60 days of the degradation, a weight loss of nearly 93% for CPR, 75% for VRCP2, and 72% for JCP2 in composting was observed. However, the weight loss in the microbial environment was considerably low as compared to the composting condition. Around 70% more degradation was reported for JCP2 in soil-burial conditions than in microbial conditions. The fungi could deteriorate the CPR, JCP2, and

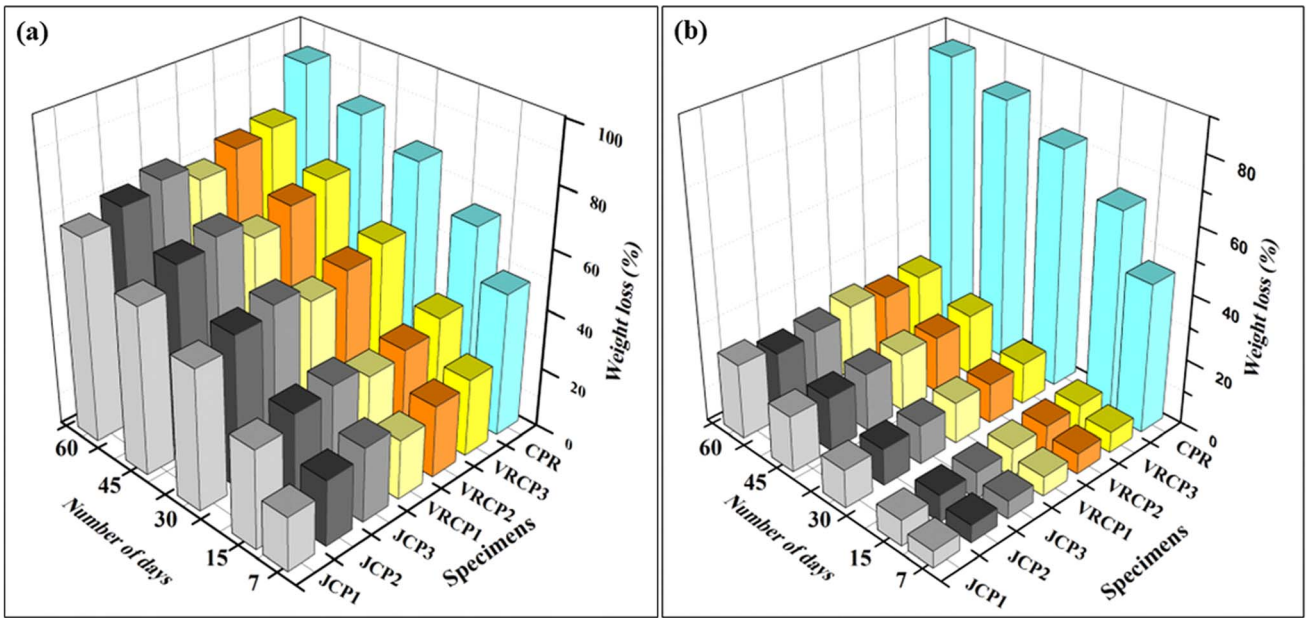

Fig. 6 Weight loss of the CPR film, JCP, and VRCP composites under (a) soil-burial condition, and (b) microbial condition.

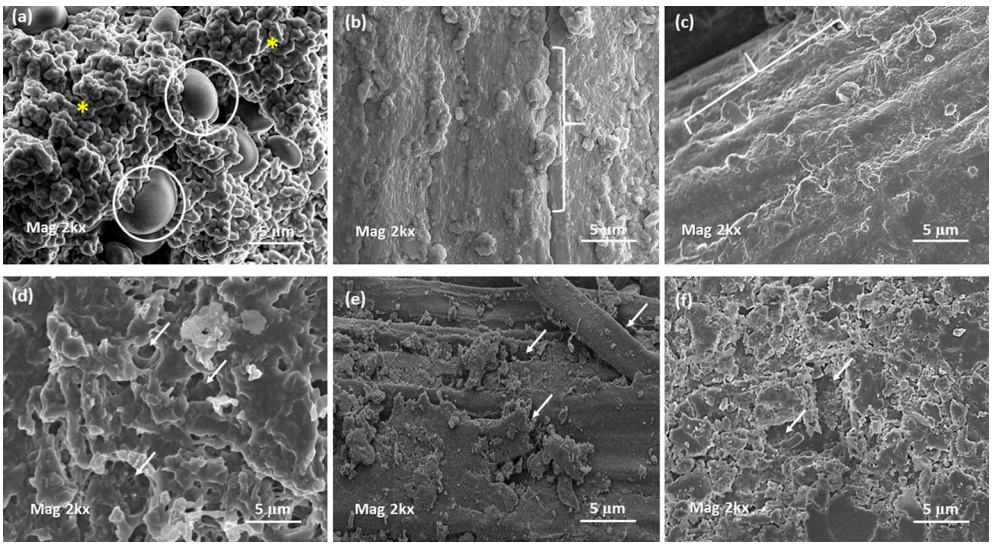

Fig. 7 Scanning electron micrographs of (a) CPR, (b) JCP2, (c) VRCP2, (d) degraded CPR, (e) degraded JCP2, and (f) degraded VRCP2. The yellow starred area is the protein matrix, whereas the circled starch molecules are dispersed in it (as shown in (a)). Curly brackets in (b and c) show the resin-coated fiber surfaces. White arrows in (d–f) mark the deteriorated surfaces of the CPR, JCP2, and VRCP2.

VRCP2 up to 85.5%, 20.54% and 21.44% of their masses, respectively.

3.8.2. Surface analysis of composites through scanning electron microscopy. Scanning electron micrographs showcasing the surface of CPR, JCP2, and VRCP2 before and after soil burial degradation are represented collectively in Fig. 7(a–f). The major presence of protein (small globular clusters) and starch molecules dispersed throughout (large oblong spheres) in the CPR matrix can be pointed out in Fig. 7(a).[14] These have been attacked by the soil microbes (Fig. 7(d)), as is evident by the destroyed surface of CPR (marked by white arrows). Long, smooth, cylindrical structures in Fig. 7(b and c) project towards the resin coated fibers of jute and vetiver in the composites, respectively. These have been withered out from the matrix post degradation (Fig. 7(e and f)).[28] The matrix shows the presence of furrows and micro-cracks, being the favoured spots of attack by the soil microbes, in comparison to the cellulosic fibers.[32]

Microbial degradation of the CPR and the JCP2 and VRCP2 composites was also analyzed under SEM imaging (Fig. 8(I)). The surface of CPR showed extensive networks of fungal hyphae growing all over the matrix (white arrows), with a thick growth of the fungi (circled particle-like structures) as seen in Fig. 8(I)

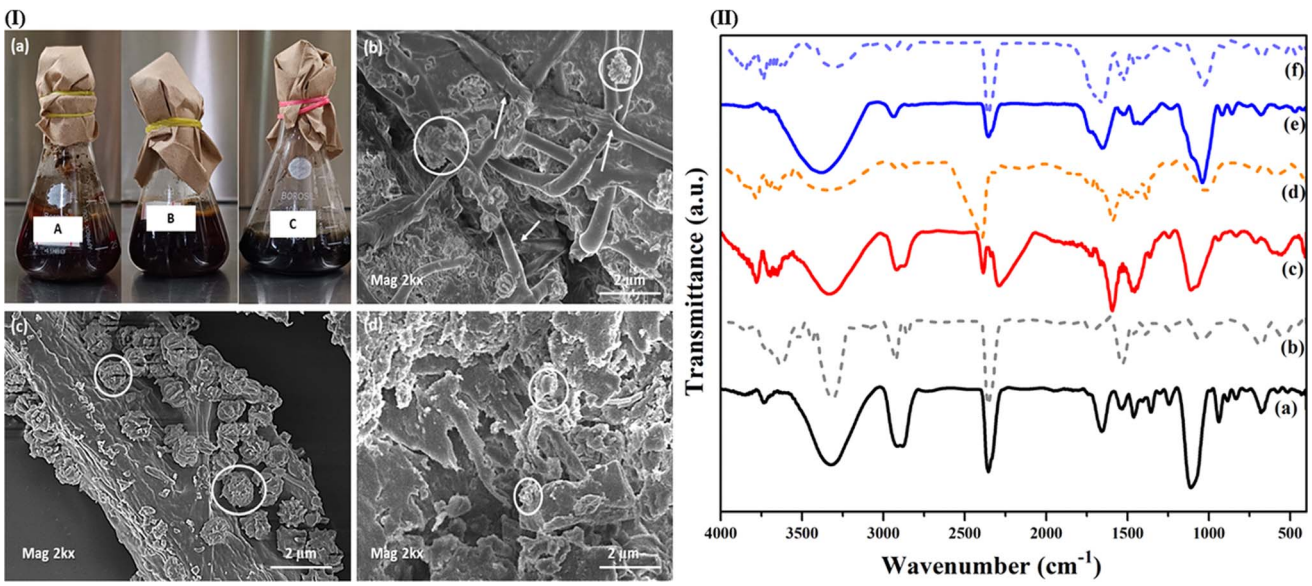

Fig. 8 (I) Representation of (a) the setup of fungal degradation in a conical flask, and post degradation SEM micrographs of (b) CPR, (c) JCP2, and (d) VRCP2. Circled structures represent *Aspergillus niger* growing on the material. Their hyphae have been marked with small arrows. (II) FTIR spectra of the pre degradation sample: (a) CPR film, (c) JCP2 composite, and (e) VRCP2 composite in comparison with their post-degradation samples in (b), (d), and (f), respectively.

(b). However in the cases of JCP2 and VRCP2 (Fig. 8(I) (c and d)), the hyphal structures were not very prominent, but the fungal particles can be seen. The destruction of the cellulosic component is a little more widespread for VRCP2 as compared to JCP2, with the defibrillation of the natural fiber.[3] For fungi too, we can conclude that the CPR resin is the preferred attacking spot being an easy protein source, which is used as a nutrient for growth.

3.8.3. Infrared spectroscopic analysis of the degraded specimens. Fig. 8II (a–f) displays the FTIR spectra of the CPR film sample and JCP2 and VRCP2 composites. The amide chains present in CPR are well viewed in Fig. 8II (a). The amide A band, which shows the N–H stretching and hydrogen-bonded O–H of starch molecules, was observed at 3331 cm^{-1}.[33] At 2921 cm^{-1}, C–H stretching of the amino acid side chains is observed. Along with that, the C═O stretching of the peptide bond peak was seen at 1655 cm^{-1}.[23] These can be seen to have diminished intensity in its degraded sample, Fig. 8II (b). Absence of –SH stretching at 2500–2600 cm^{-1} points to the absence of cysteine and methionine amino acids in cowpea protein, as mentioned in the literature.[12] In the case of JCP2 composites (Fig. 8II (c)), the constituent cellulose and hemicellulose were marked at 3341 cm^{-1}, 2912 cm^{-1}, 1601 cm^{-1}, and 1096 cm^{-1} for O–H stretching vibration, C–H stretching, C═O stretching of hemicellulose and C–O stretching of cellulose, respectively.[26] The beta-glycosidic bond between the cellulosic monomer was seen at 890 cm^{-1}. In the case of VRCP2 composites, the same peaks have little shifted values at 3369 cm^{-1}, 2949 cm^{-1}, 1665 cm^{-1}, and 1031 cm^{-1}, respectively, due to the difference in the crystallinity of the cellulose found in vetiver fiber.[23] But, for the composite, the degraded samples showed reduced intensities of these peaks and minor shifts in their positions (Fig. 8II (d and f)), suggesting the cleavage of the glycosidic and amide chains.

4. Conclusion

Cowpea resin was formulated using marked-down cowpea batches and reinforced with vetiver and jute fibers at 50, 60, and 70 weight percentages. The composites were tested for mechanical properties, with the 60 wt% fiber loading showing the best results. Tensile strengths were 37.49 MPa for JCP2 and 36.2 MPa for VRCP2, with JCP2 also displaying superior flexural properties. JCP2 exhibited a 33.38% improvement in storage modulus and a reduced tan δ by 30.6% compared to that of VRCP2. Both composites had an average Izod impact strength of 10.86 kJ m^{-2}. Tolerable hydrophilicity and dimension swelling (after water absorption) of composites made the pathway for the potential microbial degradation. Post-degradation studies, including weight loss, SEM, and FTIR, confirmed that both JCP and VRCP composites are mostly biodegradable, losing nearly 70% of their initial weight within 60 days. However, the current mechanical properties limit their use in outdoor and high-end engineering applications. Future research should focus on enhancing the mechanical properties of cowpea resin composites through alternative cross-linking agents, fiber surface treatments, and hybrid reinforcement strategies. Investigating the environmental impact and conducting life-cycle analysis will be essential for understanding the long-term sustainability of these biodegradable materials.

Data availability

The data that support the findings of this study are available from the corresponding author [Behera, A. K.] upon reasonable request.

Author contributions

Shruti S. Pattnaik: investigation, writing – original draft, visualization, conceptualization. Diptiranjan Behera: editing – original draft, formal analysis, methodology, visualization. Nigamananda Das: methodology, supervision. Ashwini K. Dash: formal analysis, conceptualization, and characterizations, Ajaya K. Behera: supervision, visualization, formal analysis, editing – original draft.

Conflicts of interest

There are no conflicts to declare.

Acknowledgements

We are very grateful to the Department of Chemistry, Utkal University, Odisha, for allowing the smooth conduct of experiments. We are also grateful to the Central Instrumentation Facility, Odisha University of Technological Research, Bhubaneswar for conducting scanning electron microscopy for the samples.

References

1 J. W. Park, S. J. Lee, D. Y. Hwang and S. Seo, Removal of microplastics *via* tannic acid-mediated coagulation and *in vitro* impact assessment, *RSC Adv.*, 2021, **11**(6), 3556–3566, DOI: 10.1039/D0RA09645H.

2 N. Tripathi, A. R. Uribe, H. Weldekidan, M. Misra and A. K. Mohanty, Upcycling of waste jute biomass to advanced biocarbon materials: the effect of pyrolysis temperature on their physicochemical and electrical properties, *Mater. Adv.*, 2022, **3**(24), 9071–9082, DOI: 10.1039/D2MA00678B.

3 A. K. Behera, S. Avancha, S. Manna, R. Sen and B. Adhikari, Effect of nanoclay on physical, mechanical, and microbial degradation of jute-reinforced, soy milk-based nano-biocomposites, *Polym. Eng. Sci.*, 2014, **54**(2), 345–354, DOI: 10.1002/pen.23556.

4 S. Nagaraja, P. B. Anand, H. D. Shivakumar and M. I. Ammarullah, Influence of fly ash filler on the mechanical properties and water absorption behaviour of epoxy polymer composites reinforced with pineapple leaf fiber for biomedical applications, *RSC adv.*, 2024, **14**(21), 14680–14696, DOI: 10.1039/D4RA00529E.

5 E. Álvarez-Castillo, M. Felix, C. Bengoechea and A. Guerrero, Proteins from agri-food industrial biowastes or co-products and their applications as green materials, *Foods*, 2021, **10**(5), 981, DOI: 10.3390/foods10050981.
6 Y. Gao, H. Zheng, J. Wang, J. Wu, X. Li and G. Liu, Physicochemical properties of zein films cross-linked with glutaraldehyde, *Polym. Bull.*, 2022, **79**(7), 4647–4665, DOI: 10.1007/s00289-021-03723-9.
7 S. Ahammed, F. Liu, M. N. Khin, W. H. Yokoyama and F. Zhong, Improvement of the water resistance and ductility of gelatin film by zein, *Food Hydrocolloids*, 2020, **105**, 105804, DOI: 10.1016/j.foodhyd.2020.105804.
8 V. Guna, F. Touchaleaume, B. Saulnier, Y. Grohens and N. Reddy, Sustainable bioproducts through thermoplastic processing of wheat gluten and its blends, *J. Thermoplast. Compos. Mater.*, 2023, **36**(4), 1775–1806, DOI: 10.1177/08927057211048540.
9 J. Li, F. Ren, X. Liu, G. Chen, X. Li, Y. Qing, Y. Wu and M. Liu, Eco-friendly fiberboards with low formaldehyde content and enhanced mechanical properties produced with activated soybean protein isolate modified urea-formaldehyde resin, *Eur. Polym. J.*, 2024, **210**, 113002, DOI: 10.1016/j.eurpolymj.2024.113002.
10 FAO, Crop Production and Trade Data, 2021, http://www.fao.org/faostat/en/#data/QC.
11 N. S. Affrifah, R. D. Phillips and F. K. Saalia, Cowpeas: Nutritional profile, processing methods and products—A review, *Legume Sci.*, 2022, **4**(3), e131, DOI: 10.1002/leg3.131.
12 A. Baptista, O. Pinho, E. Pinto, *et al.*, Characterization of protein and fat composition of seeds from common beans (*Phaseolus vulgaris L.*), cowpea (*Vigna unguiculata L. Walp*) and bambara groundnuts (*Vigna subterranea L. Verdc*) from Mozambique, *J. Food Meas. Charact.*, 2017, **11**, 442–450, DOI: 10.1007/s11694-016-9412-2.
13 USDA, Food Data Central, 2021, https://fdc.nal.usda.gov/.
14 B. A. Acevedo, M. Villanueva, M. G. Chaves, M. V. Avanza and F. Ronda, Modification of structural and physicochemical properties of cowpea (*Vigna unguiculata*) starch by hydrothermal and ultrasound treatments, *Food Hydrocolloids*, 2022, **124**, 107266, DOI: 10.1016/j.foodhyd.2021.107266.
15 R. Horax, N. S. Hettiarachchy, P. Chen and M. Jalaluddin, Preparation and characterization of protein isolate from cowpea (*Vigna unguiculata L. Walp.*), *J. Food Sci.*, 2004, **69**(2), fct114–fct118, DOI: 10.1111/j.1365-2621.2004.tb15500.x.
16 S. Hewage and S. Vithanarachchi, Preparation and characterization of biodegradable polymer films from cowpea (Vigna unguiculata) protein isolate, *J. Natl. Sci. Found. Sri Lanka*, 2009, **37**, DOI: 10.4038/jnsfsr.v37i1.457.
17 E. N. Anosike-Francis, P. A. Ubi, I. I. Obianyo, G. M. Kalu-Uka, A. Bello, M. I. Ofem, A. O. Olorunnisola and A. P. Onwualu, Mechanical and Thermomechanical Properties of Clay-Cowpea (Vigna Unguiculata Walp.) Husks Polyester Bio-Composite for Building Applications, *Appl. Sci.*, 2022, **12**(2), 713, DOI: 10.3390/app12020713.
18 X. Zhao, P. Li, F. Mo, Y. Zhang, Z. Huang, J. Yu, L. Zhou, S. Bi and S. Peng, Copolyester toughened poly (lactic acid) biodegradable material prepared by *in situ* formation of polyethylene glycol and citric acid, *RSC adv.*, 2024, **14**(16), 11027–11036, DOI: 10.1039/D4RA00757C.
19 Q. Ma, D. Mohawk, B. Jahani, X. Wang, Y. Chen, A. Mahoney, Y. Zhu and L. Jiang, UV-curable cellulose nanofiber-reinforced soy protein resins for 3D printing and conventional molding, *ACS Appl. Polym. Mater.*, 2020, **2**(11), 4666–4676, DOI: 10.1021/acsapm.0c00717.
20 A. K. Behera, C. Mohanty, S. K. Pradhan and N. Das, Assessment of soil and fungal degradability of thermoplastic starch reinforced natural fiber composite, *J. Polym. Environ.*, 2021, **29**, 1031–1039, DOI: 10.1007/s10924-020-01944-z.
21 P. Yin, X. Dong, W. Zhou, D. Zha, J. Xu, B. Guo and P. Li, A novel method to produce sustainable biocomposites based on thermoplastic corn-starch reinforced by polyvinyl alcohol fibers, *RSC adv.*, 2020, **10**(40), 23632–23643, DOI: 10.1039/D0RA04523C.
22 A. K. Behera, S. Avancha, R. K. Basak, R. Sen and B. Adhikari, Fabrication and characterizations of biodegradable jute reinforced soy based green composites, *Carbohydr. Polym.*, 2012, **88**(1), 329–335, DOI: 10.1016/j.carbpol.2011.12.023.
23 S. S. Pattnaik, S. K. Mohapatra, C. Mohanty, A. K. Behera and B. C. Tripathy, Influence of Waste Vetiver Root Fiber on Mechanical, Hydrophobicity, and Biodegradation of Soy-Based Biocomposites as Plastic Substitute, *Fibers Polym.*, 2023, **24**(1), 265–274, DOI: 10.1007/s12221-023-00085-z.
24 A. Amjad, A. Anjang and M. S. Z. Abidin, Effect of nanofiller concentration on the density and void content of natural fiber-reinforced epoxy composites. Biomass Convers, *Biomass Convers. Biorefin.*, 2024, **14**(7), 8661–8670, DOI: 10.1007/s13399-022-02839-w.
25 A. Hyde, J. He, X. Cui, J. Lua and L. Liu, Effects of microvoids on strength of unidirectional fiber-reinforced composite materials, *Composites, Part B*, 2020, **187**, 107844, DOI: 10.1016/j.compositesb.2020.107844.
26 D. Behera, S. S. Pattnaik, P. P. Mishra, R. Sahu, S. Manna, N. Das, M. Misra, A. K. Mohanty and A. K. Behera, Fabrication and characterization of industrial biocomposite from cellulosic fibers of Luffa cylindrica in a protein based natural matrix, *Ind. Crops Prod.*, 2024, **212**, 118328, DOI: 10.1016/j.indcrop.2024.118328.
27 M. A. S. Sujon, M. A. Habib and M. Z. Abedin, Experimental investigation of the mechanical and water absorption properties on fiber stacking sequence and orientation of jute/carbon epoxy hybrid composites, *J. Mater. Res. Technol.*, 2020, **9**(5), 10970–10981, DOI: 10.1016/j.jmrt.2020.07.079.
28 A. K. Behera, R. Sen and B. Adhikari, Environment-friendly fully biodegradable jute-poly (vinyl alcohol) modified soy composite development as plastic substitute, *J. Nat. Fibers*, 2022, **19**(3), 905–914, DOI: 10.1080/15440478.2020.1764440.
29 J. P. R. G. D. Carvalho, N. T. Simonassi, F. P. D. Lopes, S. N. Monteiro and C. M. F. Vieira, Novel sustainable castor oil-based polyurethane biocomposites reinforced

with piassava fiber powder waste for high-performance coating floor, *Sustain*, 2022, **14**(9), 5082, DOI: **10.3390/su14095082**.

30 S. S. Pattnaik, D. Behera, P. Jali and A. K. Behera, Mechanical and biodegradation analysis under various environmental conditions of the waste vetiver root fiber reinforced soy composite, *Polym. Int.*, 2024, DOI: **10.1002/pi.6664**.

31 N. Nurazzi, M. R. M. Asyraf, M. Rayung, M. N. F. Norrrahim, S. S. Shazleen, M. S. A. Rani, A. R. Shafi, H. A. Aisyah, M. A. H. Radzi, F. A. Sabaruddin, R. A. Ilyas, E. S. Zainudin and K. Abdan, Thermogravimetric analysis properties of cellulosic natural fiber polymer composites: A review on influence of chemical treatments, *Polym*, 2021, **13**(16), 2710, DOI: **10.3390/polym13162710**.

32 A. K. Behera and S. Manna, Evaluation of conductivity and mechanical properties of natural fiber reinforced soy-melamine formaldehyde based green composite, *Polym. Compos.*, 2022, **43**(3), 1546–1556, DOI: **10.1002/pc.26475**.

33 O. J. Ibukun, M. Gumtya, S. Singh, A. Shit and D. Haldar, Effect of the spacer on the structure and self-assembly of FF peptide mimetics, *Soft Mater.*, 2023, **19**(17), 3215–3221, DOI: **10.1039/d3sm00339f**.